JACS
JOURNAL OF THE AMERICAN CHEMICAL SOCIETY

COMMUNICATION

pubs.acs.org/JACS

Concerted Electron−Proton Transfer (EPT) in the Oxidation of Tryptophan with Hydroxide as a Base

Christopher J. Gagliardi, Robert A. Binstead, H. Holden Thorp, and Thomas J. Meyer*

Department of Chemistry, University of North Carolina at Chapel Hill, North Carolina 27599-3290, United States

Supporting Information

ABSTRACT: Tryptophan is unique among the redox-active amino acids owing to its weakly acidic indolic proton ($pK_a \approx 16$) compared to the −O−H proton of tyrosine ($pK_a = 10.1$) or the −S−H proton of cysteine ($pK_a = 8.2$). Stopped-flow and electrochemical measurements have been used to explore the roles of proton-coupled electron transfer and concerted electron−proton transfer (EPT) in tryptophan oxidation. The results of these studies have revealed a role for OH^- as a proton acceptor base in EPT oxidation of *N*-acetyl-tryptophan but not for other common bases. The reorganizational barrier for $(N\text{-acetyl-tryptophan})^{+/\bullet}$ self-exchange is also estimated.

The amino acids tyrosine, cysteine, and tryptophan play important roles as electron transfer (ET) carriers and mediators in biology, with important examples appearing in photosystem II, class I ribonucleotide reductase, and DNA photolyase.[1−8] In tyrosine and cysteine oxidation, proton-coupled electron transfer (PCET) is important in avoiding charge buildup. Concerted electron−proton transfer (EPT) pathways are used to avoid high-energy protonated intermediates that arise from ET.[9] As an example, $E^{o\prime} \approx 1.5$ V vs NHE for tyrosine oxidation to $TyrOH^{+\bullet}$, while $E^{o\prime} \approx 1.0$ V for TyrOH-histidine oxidation to $TyrO^{\bullet}$-$^{+}$H-histidine, which is important in photosystem II.[3,4] In proteins, pendant bases or solvent molecules have been suggested to act as EPT proton acceptors as a way of avoiding high-energy intermediates such as $TyrOH^{+\bullet}$. Protein structures with redox-active tyrosine residues typically include an associated histidine base and, for cysteine oxidation, a carboxylate base such as aspartate.[3,4,10,11]

EPT is utilized in tyrosine oxidation by $M(bpy)_3^{3+}$ (M = Fe, Ru, Os) with added bases by the multiple-site electron−proton transfer (MS-EPT) pathway in eq 1.[12−14] In this pathway EPT

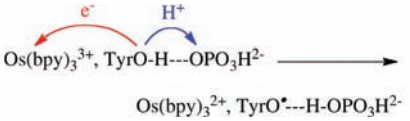

(1)

occurs, but to different e^- and H^+ acceptors. Related observations have been made at indium tin oxide (ITO, Sn(IV)-doped In_2O_3) electrodes derivatized by surface binding of the ET mediator $[Ru^{II}(bpy)(4,4'\text{-}(HO)_2P(O)CH_2)_2bpy)_2]^{2+}$ (bpy = 2,2′-bipyridine; 4,4′-$(HO)_2P(O)CH_2)_2$bpy = 4,4′-bis-methylenephosphonato-2,2′-bipyridine)[12,13] and in oxidation of the related solution complex *cis*-$Os^{III}(bpy)_2(py)(OH)^{2+}$ to $Os^{IV}(bpy)_2(py)(O)^{2+}$.[15]

In contrast to tyrosine ($pK_a = 10.1$) and cysteine ($pK_a = 8.2$), with readily dissociable protons, tryptophan is a secondary amine ($pK_a \approx 16-17$), with $E^{o\prime}(TrpNH^{+\bullet}/TrpNH) = 1.21$ V (vs NHE)[16] and $pK_a(TrpNH^{+\bullet}) = 4.3$.[17] The difference in pK_a values between radical cation and neutral is comparable for the two ($pK_a(TryOH^{+\bullet}) = -2$), as are EPT driving forces for $TrpNH^{+\bullet}$ and $TyrOH^{+\bullet}$, with $\sim 0.059(\Delta pK_a) \approx 0.7$ eV. Mitigating against EPT oxidation of tryptophan is the fact that EPT pathways are microscopically more complex than ET, with higher barriers due to the transferring proton. All things being equal, ET is expected to be favored over EPT.[18]

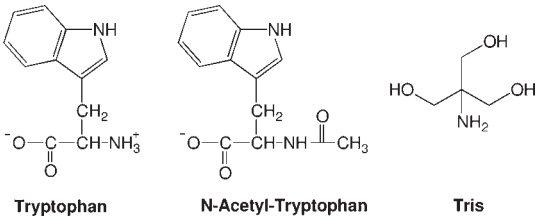

Figure 1. Structures of tryptophan and *N*-acetyl-tryptophan at neutral pH and the Tris base, 2-amino-2-(hydroxymethyl)propane-1,3-diol.

The lack of an easily dissociable proton for tryptophan has important consequences in biological ET. In peptides, tryptophan is often found in solvent-exposed sites without an associated base, suggesting that EPT may not play a role. Tryptophan has been shown to act as an ET carrier in DNA photolyase, class I ribonucloeotide reductase, and azurin proteins.[1,2,5,7,19]

The role of EPT in tryptophan oxidation remains an open question. Evidence for buffer base and pH effects in oxidation of a tryptophan derivative in a $Ru(bpy)_3^{3+}$-based molecular assembly has been observed under certain conditions by Hammarström and co-workers by use of laser flash photolysis.[20,21]

We report here oxidation of *N*-acetyl-tryptophan (NAceTrpNH, Figure 1), as a model for tryptophan in peptides, by the homologous series of polypyridyl metal complex oxidants $M(bpy)_3^{3+}$ (M = Fe, Ru, Os), analyzed by a combination of stopped-flow spectrophotometry and catalytic cyclic voltammetry (CV). An important finding, consistent with tryptophan as an ET mediator, is a failure to observe EPT pathways with a variety of acceptor bases. The only exception is OH^-, which facilitates tryptophan oxidation by MS-EPT and not by prior deprotonation of NAceTrpNH and oxidation of the anion. We also report a detailed kinetic analysis that provides an independent estimate of $E^{o\prime}$ for the $(TrpNH^{+\bullet}/TrpNH)$ couple and an estimate of the reorganization barrier to ET.

Stopped-flow mixing with diode array optical monitoring (375−775 nm) was applied to the oxidation of NAceTrpNH

Received: August 5, 2011
Published: October 27, 2011

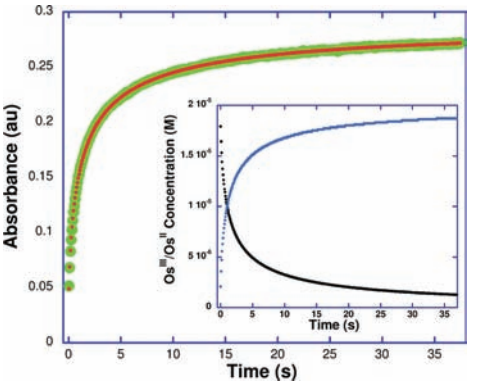

Figure 2. Typical kinetic trace at 480 nm (green) and fit (red) for the reaction of $Os(bpy)_3^{3+}$ (20 μM) with *N*-acetyl-tryptophan (200 μM) at $T = 20$ °C, pH 7.1, 40 mM Tris buffer (10:1 acid/base), $I = 0.8$ M NaCl). The inset shows the calculated concentration profiles for Os^{III} (black) and Os^{II} (blue) only. The relative error of individual fits averaged 0.55% (<0.001 au).

Scheme 1

$$Os(bpy)_3^{3+} + TrpNH \underset{k_{-1}}{\overset{k_1}{\rightleftharpoons}} Os(bpy)_3^{2+} + TrpNH^{+\bullet}$$

$$TrpNH^{+\bullet} \underset{k_{-2}}{\overset{k_2}{\rightleftharpoons}} TrpN^{\bullet} + H^+$$

$$TrpNH^{+\bullet} + TrpN^{\bullet} \xrightarrow{k_3} TrpNH + TrpN^+$$

$$TrpN^+ \xrightarrow{H_2O/O_2} oxidation\ products$$

by $Os(bpy)_3^{3+}$, $E^{o\prime}(Os^{3+/2+}) = 0.80$ V vs NHE. The oxidant was generated *in situ* by Cl_2 oxidation followed by an argon purge. The kinetics were monitored by the appearance of the $Os(bpy)_3^{2+}$ metal-to-ligand charge-transfer absorption band at λ_{max} = 480 nm following rapid mixing with solutions containing NAceTrpNH under various conditions.

Stopped-flow kinetic absorbance−time traces (Figure 2) were well modeled in SPECFIT/32 by the mechanism in Scheme 1. The key features in the mechanism are (a) a reversible $1e^-$ redox pre-equilibrium with the protonated radical cation,[22] where $E^{o\prime}$-($TrpNH^{+\bullet}$/TrpNH) is 1.21 V vs NHE for tryptophan[16] and ~1.1 V for NAceTrpNH,[23] (b) proton-transfer equilibration of the radical cation with the buffer medium to give the neutral radical at pH 7.1, and (c) reaction of the neutral radical with the protonated radical cation ($pK_a = 4.3$)[16,17] to form TrpNH and the cationic form as initial products. The assumed stoichiometry of 2:1 Os(III)/NAceTrpNH is in good agreement with previous reports at neutral pH.[16,20,24] The ultimate product(s) were not investigated, but oxidation products reported earlier for tryptophan include *N*-formylkynurenine, oxindolylalanine, and dioxindolylalanine, whose structures are shown in Figure SI.7.[16,25,26]

For Scheme 1, we have used fixed rate constants for k_2, k_{-2}, and k_3 based on pulse radiolysis studies for native tryptophan, where $pK_a = 4.3$ for the radical cation ($TrpNH^{+\bullet}$) and the disproportionation rate constant $k_3 = 3.2 \times 10^8$ M^{-1} s^{-1}.[17] Assuming diffusion-controlled protonation of the free radical, $k_{-2} = 1 \times 10^{10}$ M^{-1} s^{-1}, gives $k_2 = 5 \times 10^5$ M^{-1} s^{-1}. Based on these values and the kinetic model in Scheme 1, fits to the stopped-flow kinetic data were made with two adjustable parameters, the rate constants for the reversible pre-equilibrium, k_1 and k_{-1}. The resulting fits at pH 7.1 (40 mM Tris) gave $k_1 = (5.1 \pm 0.2) \times 10^3$ M^{-1} s^{-1}, $k_{-1} = (2.3 \pm 0.2) \times 10^8$ M^{-1} s^{-1}, and $K_{eq} = k_1/k_{-1} = 2.2 \times 10^{-5}$. Similar results

Scheme 2

$$TrpNH + OH^- \rightleftharpoons TrpN^- + H_2O : K_a/K_w$$

$$TrpN^- + Os(bpy)_3^{3+} \xrightarrow{k_{2(OH^-)}} TrpN^{\bullet} + Os(bpy)_3^{2+}$$

$$TrpN^{\bullet} \longrightarrow oxidation\ products$$

were obtained over the pH range 6.10−9.16 (see Supporting Information).

$$\Delta E^{o\prime} = E_{ox}(NAceTrp^{+\bullet/0}) - E_{ox}(M^{III/II}) = 0.059pK_{eq} \qquad (2)$$

The fitted value of K_{eq}, eq 2, gives $\Delta E^{o\prime} = 0.28$ V for oxidation of NAceTrpNH by $Os(bpy)_3^{3+}$. Given $E^{o\prime} = 0.80$ V for the $Os(bpy)_3^{3+/2+}$ couple[12,14] results in $E^{o\prime} = 1.08$ V vs NHE for the couple $TrpNH^{+\bullet}$/TrpNH. This agrees well with the electrochemically measured value of $E^{o\prime} = 1.06$ V.[23]

There was no evidence in either the stopped-flow or CV measurements (see below) for rate enhancements with added phosphate ($H_2PO_4^-/HPO_4^{2-}$) or Tris over extended concentration ranges. For example, addition of pH 7.1 Tris ($pK_a = 8.1$, 0.5−400 mM) had no effect on the rate of oxidation of NAceTrpNH by $Os(bpy)_3^{3+}$ (Table SI.2).

The role of OH^- as base was investigated over the pH range 10.00−11.94, $[OH^-] = 0.10$−8.9 mM without added buffer (I = 0.8 M, NaCl, $T = 20$ °C). Under pseudo-first-order conditions, the rate law was first order in both NAceTrpNH and OH^-. Plots of $k_{obs}/[NAceTrp]$ vs $[OH^-]$ (Figure SI.4) and $k_{obs}/[OH^-]$ vs [NAceTrp] were linear (Figure SI.4), consistent with the rate law in eq 3. From the slopes of these plots, $k_{OH^-} = (7.5 \pm 0.9) \times 10^8$ M^{-2} s^{-1} (Table SI.1).

$$rate = k_{obs}[Os(bpy)_3^{3+}]; \quad k_{obs} = k_{OH^-}[TrpNH][OH^-] \qquad (3)$$

A mechanism involving initial deprotonation of TrpNH ($pK_a \approx 16$) followed by oxidation of the anion by $Os(bpy)_3^{3+}$ (Scheme 2) can be ruled out on kinetic grounds. In this case, $k_{obs} = (K_a/K_w)k_{2(OH^-)}[TrpNH][OH^-]$, with $K_a/K_w \approx 10^{-2}$, from which $k_{2(OH^-)} = 8 \times 10^{10}$ M^{-1} s^{-1}. This value exceeds the diffusion-controlled limit under these conditions by a factor of ~5.[27]

Oxidation of NAceTrpNH by $Os(bpy)_3^{3+}$ was also investigated by stopped-flow kinetic measurements in OD^-/D_2O with NAceTrpNH varied from 200 to 500 μM at pH = pD = 11 (in D_2O, pD = pH meter reading + 0.4) (Figure SI.5). Analysis of these data gave $k_{OD^-} = (5.4 \pm 0.5) \times 10^7$ M^{-2} s^{-1} and a solvent kinetic isotope effect (KIE) of $k_{H_2O}/k_{D_2O} = 13.8 \pm 0.9$. This value is considerably in excess of typical solvent KIEs for outer-sphere ET reactions, which fall in the range 1.0−2.8.[28] There is precedence for large KIEs in biological oxidations, with k_{C-H}/k_{C-D} values in excess of 80 reported for the oxidation of linoleic acid by soybean lipoxygenase by Klinman and co-workers.[29]

As shown in Scheme 3, an alternate mechanism, consistent with the observed rate law and isotope effect, is MS-EPT with prior H-bond association between OH^- and NAceTrpNH, followed by MS-EPT analogous to eq 1. In the MS-EPT step, ET occurs to $Os(bpy)_3^{3+}$ in concert with indolic N−H proton transfer to OH^-. The magnitude of this KIE is considerably greater than the value of $k_{H_2O}/k_{D_2O} = 2.8$ observed for oxidation of tyrosine by $Os(bpy)_3^{3+}$ with acetate ($CH_3CO_2^-$) as the acceptor base.[30] A larger KIE for secondary amine oxidation is expected qualitatively owing to a less symmetric H-bond in the ion-pair adduct between the base and NAceTrpNH, resulting in a

dx.doi.org/10.1021/ja207379n |*J. Am. Chem. Soc.* 2011, 133, 19594–19597

Scheme 3

$$TrpN-H+OH^- \underset{}{\overset{K_A}{\rightleftharpoons}} TrpN-H--OH^-$$

$$Os(bpy)_3^{3+} + TrpN-H--OH^- \overset{K_A'}{\rightleftharpoons} \{Os(bpy)_3^{3+}, TrpN-H--OH^-\}$$

$$\{Os(bpy)_3^{3+}, TrpN-H--OH^-\} \xrightarrow{k_{EPT}} Os(bpy)_3^{2+} + TrpN^{\bullet} + H_2O$$

$$TrpN^{\bullet} \longrightarrow \text{oxidation products}$$

longer proton tunneling distance.[31] As noted by Savéant and coworkers, a concerted reaction is most competitive with stepwise pathways at the midpoint between pK_a values for the oxidized ($TrpNH^{+\bullet/0}$) and reduced (TrpNH) forms of the couple.[15] This is the case for MS-EPT oxidation with OH^- as base under our conditions, with $\Delta pK_a/2 \approx 10-11$.

Stoichiometric oxidation of NAceTrpNH by $Os(bpy)_3^{3+}$ under 1:1 conditions at pH 10.7 gave excellent fits to second-order, equal concentration kinetics (Figure SI.3). This is consistent with a mechanism in which $Os(bpy)_3^{3+}$ reacts only with NAceTrpNH without complications from further oxidation of $TrpN^{\bullet}$ or $TrpNH^{+\bullet}$. Under identical conditions with a 2:1 ratio of Os(III):NAceTrpNH, only 1 equiv of $Os(bpy)_3^{3+}$ was reduced on the stopped-flow time scale, in agreement with the known one-electron stoichiometry for oxidation of tryptophan at high pH.[16,20]

We also investigated electrochemical oxidation of NAceTrpNH in 50 mM Tris buffer (pH 7.1, I = 0.8 M NaCl) by CV measurements. As for other small organic molecules, TrpNH has a kinetically slow response at ITO electrodes, with only small currents in excess of the background observed near the solvent oxidation limit (Figure 3, inset). In the presence of a suitable redox mediator, much larger catalytic currents were observed (Figure 3), with rate information available by simulation of CV waveforms.[14] We investigated the influence of NAceTrpNH on catalysis of the $M(bpy)_3^{2+} \rightarrow (e^-)$ $M(bpy)_3^{3+}$ wave for the redox couples $M(bpy)_3^{3+/2+}$ (M = Fe, Os), $M(dmb)_3^{3+/2+}$ (M = Fe, Ru), and $Ru(dmb)_2(bpy)^{3+/2+}$ (dmb = 4,4′-dimethyl-2,2′-bipyridine), with $E^{o\prime}$ values ranging from 0.8 to 1.13 V vs NHE (Table 1). All of these couples are electrochemically reversible.[14]

Analysis of catalytic currents was performed by numerical simulations with DigiSim (Bioanalytical Systems, Inc.). The mechanism in Scheme 1 was used to model the waveforms. In the simulations there were two adjustable parameters: k_s, the rate of heterogeneous ET at the electrode for oxidation of $M(bpy)_3^{2+}$, and k_1, the rate constant for oxidation of TrpNH by $M(bpy)_3^{3+}$. The value of k_1 was varied to obtain the best fit to the waveforms, with k_{-1} determined by the equilibrium ratio, $k_1/k_{-1} = K_{eq} = \exp -\{(E^{o\prime}(M^{3+/2+}) - (E^{o\prime}(TrpNH^{+\bullet/0})/0.026\}$, and $E^{o\prime}(TrpNH^{+\bullet/0})$ = 1.06 V. Diffusion coefficients used in the simulations were either measured or reported previously.[14] Further details about the simulations can be found in the Supporting Information. The electrochemical model produced satisfactory fits to the cyclic voltammograms, providing rate constants for outer-sphere ET, k_1 (Figure SI.16) and $k_1 = k_{ET}K_a$ (Scheme 4). The results are summarized in Table 1, together with $E^{o\prime}$ values for the $M(bpy)_3^{3+/2+}$ couples and $\Delta G^{o\prime}$ values for oxidation of NAceTrpNH. For $Os(bpy)_3^{3+}$ as oxidant, there was no significant catalytic current, and the rate constant obtained by stopped-flow measurements is reported in Table 1.

With 0.5−500 mM added Tris buffer (pK_a = 8.1, 10:1 acid/base) and $Ru(dmb)_3^{3+}$ as the electrocatalyst, there was no sign of enhanced current response from the added base (Figure SI.13). Furthermore, k_{H_2O}/k_{D_2O} = 1.3 with NAceTrp (100 μM) + $Ru(dmb)_3^{2+}$ (20 μM) in 50 mM Tris (10:1 acid/base) at pH 7.1 (I = 0.8 M, NaCl, T = 25 ± 2 °C) with a scan rate of 300 mV/s. This behavior is in dramatic contrast to tyrosine oxidation, with significant rate enhancements observed under the same conditions.[14] The absence of significant base or isotope effects is consistent with oxidation by rate-limiting outer-sphere ET (Scheme 4).

In the classical limit, the rate constant for ET, $k_{obs} = k_{ET}K_A$ (= k_1 in Scheme 1), is given by eqs 5 and 6.

$$RT\ln k_{ET} = RT\ln k_0 + (\Delta G_{ET}/2)(1 + \Delta G_{ET}/2\lambda) \quad (5)$$

$$k_0 = \nu_{ET}K_A(4\pi RT\lambda)^{-1/2} \exp -[\lambda/4RT] \quad (6)$$

In these equations, ν_{ET} is the ET barrier crossing frequency, and ΔG_{ET} is the free energy change for the ET step, given by ΔG_{ET} (eV) = $-\{E^{o\prime}(M^{3+/2+}) - E^{o\prime}(TrpNH^{+\bullet}/TrpNH)\} - 0.059(pK_A' - pK_A)$, with K_A and K_A' the association constants for the ET reactants (4a) and products (4c), respectively. In eq 6, k_0 is the rate constant at ΔG_{ET} = 0, and λ is the sum of intramolecular (λ_i) and medium (λ_o) reorganization energies.[3,32]

Figure 4 shows a plot of $RT\ln(k_{ET})$ vs $-\Delta G^{o\prime}$ (eV), with $\Delta G^{o\prime}$ (eV) = $-\{E^{o\prime}(M^{3+/2+}) - E^{o\prime}(TrpNH^{+\bullet}/TrpNH)\}$, which neglects K_A and K_A'. A fit to eq 5 (red) is shown through the data (blue circles) with the parameters $k_0 = 1.7 \times 10^7$ M^{-1} s^{-1} and λ = 0.6. The value of k_0 was taken for the $Ru(dmb)_3^{3+/2+}$ couple with

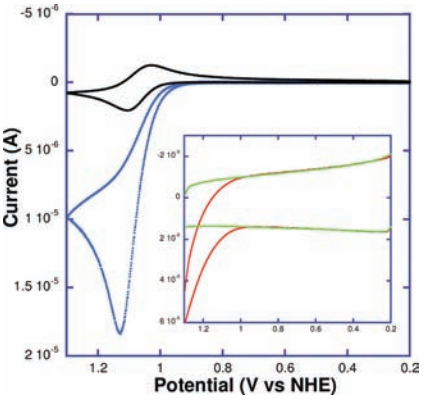

Figure 3. Cyclic voltammograms (300 mV/s) in 50 mM $H_2PO_4^-$/HPO_4^{2-} (10:1 acid/base) at pH 6.2 (I = 0.8 M, NaCl), T = 25 ± 2 °C, for (a) ITO only (green, inset); (b) ITO + NAceTrp (100 μM, red, inset); (c) ITO + $Ru(dmb)_3^{2+}$ (20 μM, black); (d) ITO + NAceTrp (100 μM) + $Ru(dmb)_3^{2+}$ (20 μM, blue).

Table 1. Rate Constants (k_{ET}) Obtained by Numerical Simulation of Oxidative Sweep Cyclic Voltammograms with NAceTrpNH (100 μM) + Oxidant (20 μM) in 50 mM Tris (10:1 Acid/Base) at pH 7.1 (I = 0.8 M, NaCl), T = 25 ± 2 °C, with a Scan Rate of 300 mV/s

metal mediator	$E^{o\prime}$ (V vs NHE)	ΔG° (eV)	k_{ET} (M^{-1} s^{-1})	$RT\ln(k_{ET})$ (eV)
$Ru(dmb)_2(bpy)^{3+/2+}$	1.13	−0.07	2.3×10^7	0.430
$Ru(dmb)_3^{3+/2+}$	1.06	0	1.7×10^7	0.423
$Fe(bpy)_3^{3+/2+}$	1.03	0.03	1.1×10^7	0.410
$Fe(dmb)_3^{3+/2+}$	0.86	0.2	4.4×10^4	0.269
$Os(bpy)_3^{3+/2+}$	0.80	0.26	5.6×10^{3a}	0.221

[a] Rate constants for $Os(bpy)_3^{3+/2+}$ were taken from stopped-flow experiments from kinetic analysis with SPECFIT/32.

dx.doi.org/10.1021/ja207379n |J. Am. Chem. Soc. 2011, 133, 19594–19597

Scheme 4

$$M(bpy)_3^{3+} + TrpNH \rightleftharpoons \{M(bpy)_3^{3+}, TrpNH\} \quad (4a)$$

$$\{M(bpy)_3^{3+}, TrpNH\} \xrightarrow{k_{ET}} \{M(bpy)_3^{2+}, TrpNH^{+\bullet}\} \quad (4b)$$

$$\{M(bpy)_3^{2+}, TrpNH^{+\bullet}\} \rightleftharpoons M(bpy)_3^{2+} + TrpNH^{+\bullet} \quad (4c)$$

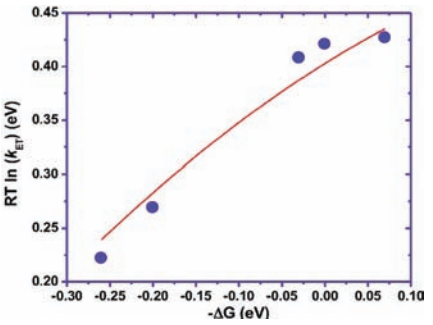

Figure 4. Variation of $RT\ln(k_{ET})$ vs $-\Delta G^{\circ\prime}$ (eV) for outer-sphere ET between *N*-acetyl-tryptophan and the oxidants $M(bpy)_3^{3+}$, from Table 1.

$E^{\circ\prime}$ = 1.06 V vs NHE, where $\Delta G^{\circ\prime} = 0$. Based on λ = 0.39 eV for $M(bpy)_3^{3+/2+}$ self-exchange and the relationship $\lambda = (\lambda_{TrpNH} + \lambda_{[M(bpy)_3]^{3+}})/2$, assuming the pre-exponential factor in eq 6 is $\nu_{ET}K_A \approx 10^{11}$ gives $\lambda_{TrpNH} \approx 0.8$ eV.[33,34]

Our results are consistent with a role for the $TrpNH^{+\bullet}$/TrpNH couple as an ET entryway and mediator in biological ET with no evidence for EPT pathways except for OH^- as acceptor base. Tryptophan benefits from a relatively small reorganization barrier, enabling it to facilitate ET. Given its relatively high pK_a, EPT pathways are relatively noncompetitive with ET, with the exception of OH^-, which is the most powerful proton acceptor base available in water as solvent.

■ ASSOCIATED CONTENT

Supporting Information. Experimental details and analyses. This material is available free of charge via the Internet at http://pubs.acs.org.

■ AUTHOR INFORMATION

Corresponding Author
tjmeyer@email.unc.edu

■ ACKNOWLEDGMENT

This work has been supported by the National Science Foundation under grant CHE-0957215. In addition, R.A.B. was supported as part of the UNC EFRC: Solar Fuels and Next Generation Photovoltaics, and C.J.G. acknowledges partial support by the Center for Catalytic Hydrocarbon Functionalization at University of Virginia. Both are Energy Frontier Research Centers funded by the U.S. Department of Energy, Office of Science, Office of Basic Energy Sciences, under Award Numbers DE-SC0001011 and DE-SC0001298, respectively.

■ REFERENCES

(1) Aubert, C.; Vos, M. H.; Mathis, P.; Eker, A. P. M.; Brettel, B. *Nature* **2000**, *405*, 586–590.
(2) Lukacs, A.; Eker, A. P. M.; Byrdin, M.; Brettel, K.; Vos, M. H. *J. Am. Chem. Soc.* **2008**, *130*, 14394–14395.
(3) Huynh, M. H.; Meyer, T. J. *Chem. Rev.* **2007**, *107*, 5004–5064.
(4) Meyer, T. J.; Huynh, M. V.; Thorp, H. H. *Angew. Chem., Int. Ed.* **2007**, *46*, 5284–5304.
(5) Stubbe, J.; van der Donk, W. A. *Chem. Rev.* **1998**, *98*, 705–762.
(6) Reece, S.; Hodgkiss, J.; Stubbe, J.; Nocera, D. *Philos. Trans. R. Soc. London B: Biol. Sci.* **2006**, *361*, 1351.
(7) Seyedsayamdost, M, R.; Yee, C. S.; Reece, S. Y.; Nocera, D. G.; Stubbe, J. *J. Am. Chem. Soc.* **2006**, *128*, 1562–1568.
(8) Zouni, A. Z.; Witt, H.; Kern, J.; Fromme, P.; Krauss, N.; Saenger, W.; Orth, P. *Nature* **2001**, *409*, 739–743.
(9) Alternate terms for EPT from the literature include concerted proton−electron transfer (CPET) and concerted electron−proton transfer (CEP). See refs 15, 20, and 21.
(10) Persson, A. L.; Erikson, M.; Katterle, B.; Pötsch, S.; Sahlin, M.; Sjöberg, B. *J. Biol. Chem.* **1997**, *272*, 31533–31541.
(11) Ekberg, M.; Pötsch, S.; Sandin, E.; Thunnissen, M.; Nordlund, P.; Sahlin, M.; Sjöberg, B. *J. Biol. Chem.* **1998**, *273*, 21003–21008.
(12) Gagliardi, C. J.; Jurss, J. W.; Thorp, H. H.; Meyer, T. J. *Inorg. Chem.* **2011**, *50*, 2076–2078.
(13) Jurss, J. W.; Concepcion, J. C.; Norris, M. R.; Templeton, J. L.; Meyer, T. J. *Inorg. Chem.* **2010**, *49*, 3980–3982.
(14) (a) Fecenko, C. J.; Meyer, T. J.; Thorp, H. H. *J. Am. Chem. Soc.* **2006**, *128*, 11020–11021. (b) Fecenko, C. J.; Meyer, T. J.; Thorp, H. H. *J. Am. Chem. Soc.* **2007**, *129*, 15098–15099.
(15) Costentin, C.; Robert, M.; Savéant, J. M. *Proc. Natl. Acad. Sci. U.S.A.* **2009**, *106*, 11829–11836.
(16) Stewart, D. J.; Napolitano, M. J.; Bakhmutova-Albert, E. V.; Margerum, D. W. *Inorg. Chem.* **2008**, *47*, 1639–1647.
(17) Posener, M. L.; Adams, G. E.; Wardman, P. *J. Chem. Soc., Faraday Trans. 1* **1976**, *72*, 2231–2239.
(18) Weinberg, D. R.; Gagliardi, C. J.; Hull, J. F.; Murphy, C. F.; Kent, C. K.; Westlake, B.; Paul, A.; Ess, D. H.; McCafferty, D. G.; Meyer, T. J. *Chem. Rev.* **2011**, submitted.
(19) Shih, C.; Museth, A. K.; Abrahamsson, M.; Blnco-Rodriguez, A. M.; Di, Bilio, A. J.; Sudhamsu, J.; Crane, B. R.; Ronayne, K. L.; Towrie, M.; Vlček, A., Jr.; Richards, J. H.; Winkler, J. R.; Gray, H. B. *Science* **2008**, *320*, 1760.
(20) Sjödin, M.; Stenbjörn, S.; Åkermark, B.; Sun, L.; Hammarström, L. *J. Am. Chem. Soc.* **2000**, *122*, 3932–3936.
(21) Zhang, M.; Hammarström, L. *J. Am. Chem. Soc.* **2011**, *133*, 8806–8809.
(22) Jovanovic, S. V.; Harriman, A.; Simic, M. *J. Phys. Chem.* **1986**, *90*, 1935–1939.
(23) Malfoy, B.; Reynaud, J. A. *J. Electroanal. Chem.* **1980**, *114*, 213–223.
(24) Merényi, G.; Lind, J.; Shen, X. *J. Phys. Chem.* **1988**, *92*, 134–137.
(25) Ogata, N. *Biochemistry* **2007**, *46*, 4898–4911.
(26) Savige, W. E. *Aust. J. Chem.* **1971**, *24*, 1285–1293.
(27) (a) Alberty, R. A.; Hammes, G. G. *J. Phys. Chem.* **1958**, *62*, 154–159. (b) Hammes, G. G. *Principles of Chemical Kinetics*; Academic Press: New York, 1978; p 203.
(28) Weaver, M. J.; Tyma, P. D.; Nettles, S. M. *J. Electroanal. Chem.* **1980**, *114*, 53–72.
(29) (a) Rickert, K. W.; Klinman, J. P. *Biochemistry* **1999**, *38*, 12218–12228. (b) Glickman, M. H.; Klinman, J. P. *Biochemistry* **1995**, *34*, 14077–14092.
(30) Murphy, C. F. Ph.D. dissertation, University of North Carolina, Chapel Hill, NC, 2009.
(31) Iordanova, N.; Hammes-Schiffer, S. *J. Am. Chem. Soc.* **2002**, *124*, 4848–4856.
(32) Chen, P.; Meyer, T. J. *Chem. Rev.* **1998**, *98*, 1439–1477.
(33) Young, R. C.; Keene, F. R.; Meyer, T. J. *J. Am. Chem. Soc.* **1977**, *99*, 2468–2473.
(34) Marcus, R. A. *J. Phys. Chem.* **1963**, *67*, 853–857.